DOI: 10.1002/chem.201000303

A Zeolite-Supported Molecular Ruthenium Complex with η^6-C_6H_6 Ligands: Chemistry Elucidated by Using Spectroscopy and Density Functional Theory

Isao Ogino,[a] Mingyang Chen,[b] Jason Dyer,[b] Philip W. Kletnieks,[c] James F. Haw,[c] David A. Dixon,*[b] and Bruce C. Gates*[a]

Abstract: An essentially molecular ruthenium–benzene complex anchored at the aluminum sites of dealuminated zeolite Y was formed by treating a zeolite-supported mononuclear ruthenium complex, $[Ru(acac)(\eta^2\text{-}C_2H_4)_2]^+$ (acac = acetylacetonate, $C_5H_7O_2^-$), with $^{13}C_6H_6$ at 413 K. IR, ^{13}C NMR, and extended X-ray absorption fine structure (EXAFS) spectra of the sample reveal the replacement of two ethene ligands and one acac ligand in the original complex with one $^{13}C_6H_6$ ligand and the formation of adsorbed protonated acac (Hacac). The EXAFS results indicate that the supported $[Ru(\eta^6\text{-}C_6H_6)]^{2+}$ incorporates an oxygen atom of the support to balance the charge, being bonded to the zeolite through three Ru–O bonds. The supported ruthenium–benzene complex is analogous to complexes with polyoxometalate ligands, consistent with the high structural uniformity of the zeolite-supported species, which led to good agreement between the spectra and calculations at the density functional theory level. The calculations show that the interaction of the zeolite with the Hacac formed on treatment of the original complex with $^{13}C_6H_6$ drives the reaction to form the ruthenium–benzene complex.

Keywords: density functional calculations · EXAFS spectroscopy · NMR spectroscopy · ruthenium · zeolites

Introduction

Ruthenium complexes are important homogeneous catalysts for a broad range of reactions, such as hydrogenation, oxidation, C–C coupling, and alkene metathesis.[1] Many of the opportunities offered by ruthenium complexes as homogeneous catalysts are expected to extend to oxide-supported ruthenium complexes that are analogous to molecular species, in which the use of the support as a ligand affords the advantages of ease of separation from products and lack of corrosion.

Molecular ruthenium complexes that incorporate polyoxometalate ligands offer what appear to be the best available models of oxide-supported ruthenium complexes,[2] but the investigation of complexes with these ligands is hampered by 1) the challenge of synthesizing the complexes, which is associated with the relative inertness of the oxygen sites in polyoxometalates, and 2) the difficulty of purifying the resultant compounds. Nonetheless, some ruthenium complexes with polyoxometalate ligands have been crystallized and characterized structurally by using single-crystal X-ray diffraction,[2f–g] with results that provide a basis for determining the lengths and strengths of metal–oxygen bonds and thus allow comparisons of these bond lengths with those in ruthenium complexes on oxide supports, determined by using extended X-ray absorption fine structure (EXAFS) spectroscopy.

It remains challenging to understand the chemistry of metal complexes on supports because the intrinsic nonuniformity of most support surfaces implies that the supported species include a range of sites with various attachment points and structures. If the support is crystalline, however, the hindrance of surface nonuniformity may be largely overcome. Thus, our strategy in investigating supported rutheni-

[a] I. Ogino, Prof. B. C. Gates
Department of Chemical Engineering and Materials Science
University of California, Davis
Davis, CA, 95616 (USA)
Fax: (+1) 530-752-1031
E-mail: bcgates@ucdavis.edu

[b] M. Chen, J. Dyer, Prof. D. A. Dixon
Department of Chemistry, University of Alabama
Tuscaloosa, AL, 35487 (USA)
Fax: (+1) 205-348-4704
E-mail: dadixon@bama.ua.edu

[c] P. W. Kletnieks, Prof. J. F. Haw
Department of Chemistry, University of Southern California
Los Angeles, CA 90089 (USA)

Supporting information for this article is available on the WWW under http://dx.doi.org/10.1002/chem.201000303.

um complexes was to use a crystalline porous material with well-defined and isolated bonding sites for metal complexes as the support. We chose dealuminated HY zeolite because the results of earlier investigations showed that mononuclear metal complexes on this support have a high degree of uniformity.[3] These complexes were synthesized by reacting *cis*-[Ru(acac)$_2$(η^2-C_2H_4)$_2$] (**I**; acac = acetylacetonate, $C_5H_7O_2^-$),[3d,e] [Rh(acac)(η^2-C_2H_4)$_2$],[3a,c,f] or [Ir(acac)(η^2-C_2H_4)$_2$][3b] with the acidic sites of the zeolite support. In reactions with these precursors, the metal ion complex can displace the proton in the acidic site, and the uniformity of the resultant surface metal complexes allows precise characterization of their chemistry in the absence of complicating solvents by methods such as EXAFS, NMR, and IR spectroscopies.[3] Furthermore, the uniformity of the species allowed the use of electronic structure calculations at the DFT level to predict the potential energy surfaces and spectroscopic properties of realistic models, and a satisfying agreement between the experimental and theoretical results was found.[3c,f]

Herein, we report how the supported mononuclear ruthenium complex formed by the reaction of **I** with the zeolite can be converted into supported mononuclear ruthenium species with benzene ligands. The structures of the supported ruthenium species were determined by using EXAFS, IR, and ^{13}C NMR spectroscopies supported by electronic structure calculations at the DFT level.

The results provide, for the first time, evidence of benzene ligands bonded to Ru^{II} centers that are supported on a zeolite, and they illustrate the unique opportunities that supported metal complexes in almost-uniform arrays offer for the fundamental understanding of organometallic chemistry in the absence of solvent effects.

Results

Structural characterization of initially prepared zeolite-supported ruthenium ethene complex: In earlier work,[3d,e,g] we used IR and EXAFS spectroscopies to characterize the zeolite-supported ruthenium complex formed by the reaction of **I** with dealuminated zeolite HY. IR spectra showed that one of the acac ligands originally bonded to the Ru^{II} in **I** was removed, and the complex became bonded at an acidic Al site of the zeolite. The IR spectrum of our supported sample has bands at $\tilde{\nu}$ = 3010, 3030, and 3069 cm^{-1}, which were assigned to C–H stretching bands of π-bonded ethene.[3d] This assignment is consistent with our DFT calculations with the B3LYP exchange-correlation functional described below (Table 1, Figure 1). EXAFS data characterizing this supported ruthenium complex (Table 2) show that each Ru atom on average was bonded to two oxygen atoms at the Al sites of the zeolite, with retention of one acac ligand and two ethene ligands, as shown in Scheme 1.

To model the supported ruthenium complexes, an appropriate model cluster representing the zeolite has to be constructed. In these systems, a negatively charged acac ligand on the Ru^{II} is displaced by the anionic site of the zeolite represented by a tetrahedral Al(OR)$_4^-$. On the basis of our previous work on Rh^{I} complexes bonded to the acidic zeolite site,[3c,f] we employed two clusters as models (R = H for the simplest model; R = Si(OH)$_3$ in the anionic site for the more complex model). We investigated these sites and other models. We also performed calculations on parent complex **I** in the *cis* arrangement for comparison with the experimental crystal structure.[4] The ground states of these clusters are singlets. The comparison for the average bond lengths is as follows: r(Ru–O) = 2.094 (calcd), 2.066 Å (exptl); r(Ru–C) = 2.220 (calc), 2.202 Å (exptl); and r(C=C) = 1.387 (calcd), 1.362 Å (exptl). Thus, the calculated results agree with experiment to within 0.03 Å, and so we expect our calculated structures of the zeolite model to be of approximately the same quality.

The calculated geometries about the Ru atom for the two models of the metal complex at the zeolite acidic site are very similar, consistent with the results from our previous work.[3c,f] The overall agreement between the structure determined from the EXAFS data and the calculated model structure is good (Table 2). There is excellent agreement between the average Ru–C(η^2-C_2H_4) length determined with either model and the EXAFS results. The calculated average Ru–O lengths are 0.04 to 0.08 Å too long, with the larger model giving the bigger departure from experimental values, just as was found in our earlier works on rhodium complexes bonded to the zeolite.[3c,f] The Ru–O(acac) bond lengths are 0.08 (Figure 1a) to 0.13 Å (Figure 1b) shorter than the Ru–O(zeolite acidic site) bond lengths.

Table 1. Vibrational frequencies of the supported ruthenium complexes formed by the reaction of **I** with dealuminated zeolite Y.

Molecular species	ν_{CH} of C_2H_4 or C_6H_6 [cm^{-1}]		ν of acac ligands [cm^{-1}]	
	Calcd (scaled DFT)[a]	Exptl	Calcd (scaled DFT)	Exptl
[Ru(acac)(Al{OSi(OH)$_3$}$_4$)(C_2H_4)$_2$] (Figure 1b)	3007(×2), 3022(×2), 3092(×2), 3118(×2)	3010, 3030, 3069	1575, 1506[b]	1575, 1555, 1521
[Ru{Al(OR)$_4$}(C_6H_6)] (Figure 5a)	3083, 3085, 3091, 3096, 3101, 3109 (Av. = 3094)	3065		
[Ru{Al(OR)$_4$}(C_6H_6)] (Figure 5b)	3076, 3080, 3090, 3094, 3099, 3109 (Av. = 3091)	3065		
[Ru{Al(OR)$_4$}(C_6H_6)] (Figure 5c)	3078, 3087, 3090, 3097, 3097, 3104 (Av. = 3092)	3065		
[Ru{Al(OR)$_4$}(C_6H_6)] (Figure 5d)	3083, 3087, 3088, 3096, 3098, 3103 (Av. = 3092)	3065		
[Al(acac)$_3$]			1590, 1520[b]	1590, 1537
I	3006(×2), 3024(×2), 3088(×2), 3116(×2)		1583, 1505[b]	1576, 1515

[a] Scaled by a factor of 0.954, obtained from ν(exptl)/ν(calcd) for C_2H_4 for the C–H bonds (see Supporting Information). The same value of 0.954 is obtained for C_6H_6 from ν(exptl)/ν(calcd). [b] Scaled by a factor of 0.97, obtained from ν(exptl)/ν(calcd) for **I** (see the Supporting Information).

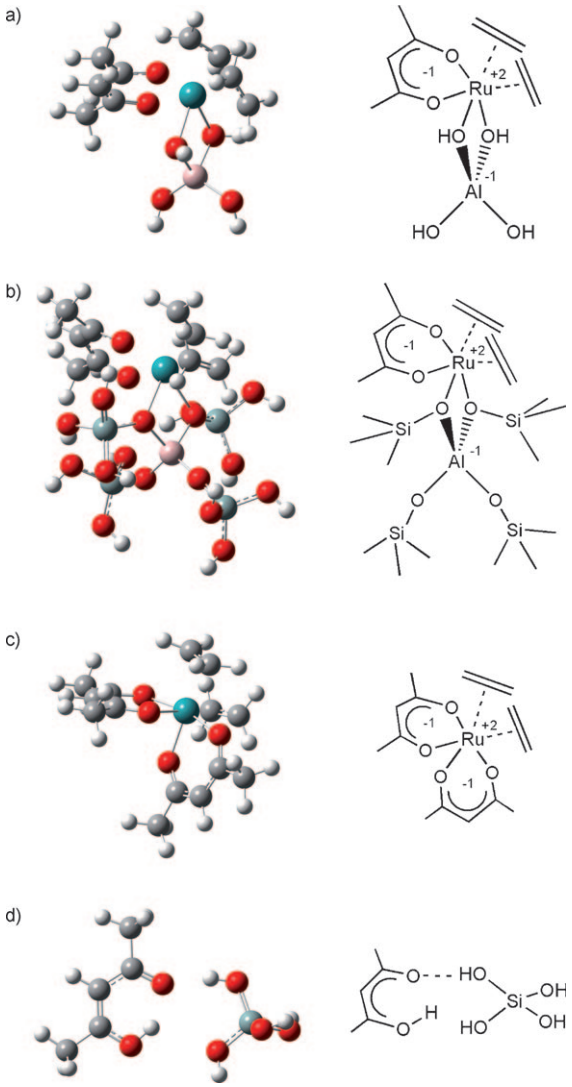

Figure 1. DFT-optimized molecular geometries for the following models: a) [Ru(acac){Al(OH)$_4$}(η^2-C_2H_4)$_2$], r(Ru–O(acac)) = 2.083, 2.060 Å, r(Ru–O(Al)) = 2.152, 2.156 Å; b) structure **II** ([Ru(acac){Al(OR)$_4$}(η^2-C_2H_4)$_2$] (R = Si(OH)$_3$), r(Ru–O(acac)) = 2.076, 2.086 Å, r(Ru–O(Al)) = 2.202, 2.217 Å; c) structure **I**, r(Ru–O(acac)) = 2.083, 2.104 Å; and d) the hydrogen-bonded complex of Hacac with Si(OH)$_4$. Red = O; white = H; pink = Al; blue = Ru; grey = C.

This comparison suggests that there is more localized negative charge on the zeolite bonding site than on the acac. The calculated Ru–Al bond length is 0.05 to 0.08 Å shorter than the experimental value. The calculated Ru–C(acac) length is in excellent agreement with experiment.

Product of the reaction of supported ruthenium ethene complex with $^{13}C_6H_6$

Treatment of the initially prepared sample with $^{13}C_6H_6$ and IR characterization of the treated sample in the ν_{CH} region: When the [Ru^{II}(acac)(η^2-C_2H_4)$_2$(zeolite)] sample described in the preceding section was exposed to $^{13}C_6H_6$ at 413 K, a reaction took place as shown by the change in color of the solid from light pink to light orange, consistent with a change in the structure of the supported ruthenium species. IR spectra of this sample demonstrate the disappearance of the ν_{CH} bands of the π-bonded ethene ligands (at $\tilde{\nu}$ = 3010, 3030, and 3069 cm^{-1}) and the appearance of a broad band centered at $\tilde{\nu}$ = 3065 cm^{-1} that is characteristic of ν_{CH} bands of $^{13}C_6H_6$ in the liquid phase[5] or bonded to ruthenium (Figure 2).[2e,g] Thus, these results indicate the removal of ethene ligands from the ruthenium and the presence of $^{13}C_6H_6$ in the sample, but they are not sufficient to distinguish physisorbed from chemisorbed $^{13}C_6H_6$.

The calculated C–H stretching frequencies are consistent with this assessment. The calculated values for the diethene complexes are in satisfactory agreement with experimental values, being up to 50 cm^{-1} too high for the higher-frequency stretches. The predicted spread in the C–H stretching frequencies for the diethene complexes is more than 110 cm^{-1}. In contrast, the predicted spread for the benzene complex is much smaller at 20 to 30 cm^{-1}, which is consistent with the experimentally observed broad band. The average for the calculated C–H frequencies for the C_6H_6 complexes is approximately 25 to 30 cm^{-1} greater than that of the center of the broad experimental band.

^{13}C CP/MAS NMR characterization of the treated sample: The ^{13}C NMR spectra clarify the nature of the supported species formed in the reaction with $^{13}C_6H_6$. The spectrum includes two resonances at δ = 93 and 122 ppm (Figure 3). The sharp resonance at δ = 122 ppm almost matches that characteristic of $^{13}C_6H_6$ in the liquid phase, at δ = 128.4 ppm[6] and is, therefore, attributed to physisorbed $^{13}C_6H_6$ in the zeolite pores. The resonance at δ = 93 ppm is consistent with the presence of $^{13}C_6H_6$ bonded to the sample; we infer that these ligands are bonded to Ru atoms, as our earlier investigation of zeolite-supported rhodium complexes by ^{13}C NMR spectroscopy indicated a chemical shift characteristic of $^{13}C_6H_6$ bonded to Rh at δ = 104 ppm, an upfield shift consistent with complexation to rhodium metal.[3c]

The calculated ^{13}C chemical shifts provide further support for this assignment. The calculated ^{13}C chemical shift for gas-phase C_6H_6 is δ = 133.5 ppm, in good agreement with the value for C_6H_6 in the liquid phase. The average chemical shifts characterizing the C_6H_6 range from δ = 84 to 86 ppm for the four structures discussed below, consistent with our assignment of the peak at δ = 93 ppm to a benzene molecule bonded to Ru at the acidic site of the zeolite.

To confirm the quality of the calculations, we calculated the chemical shifts for the ethenes in **I**. The average calculated ^{13}C chemical shift for ethene is δ = 85.4 ppm in comparison with the experimental value of δ = 78.2 ppm,[4] consistent with our previous calculations of such shifts.[3c,f]

IR characterization of the treated sample in the $\tilde{\nu}$ = 1500–1600 cm^{-1} region: The IR data characterizing this sample (Figure 4) exhibit an almost complete disappearance of the bands characteristic of the acac ligands on ruthenium prior to the treatment with $^{13}C_6H_6$ (bands at $\tilde{\nu}$ = 1521, 1555, and

Table 2. EXAFS parameters at the Ru K edge for zeolite-supported ruthenium complex samples and Ru–X interatomic distances calculated by DFT.

Sample	Backscatterer	N[a]	$\Delta\sigma^2\times10^3$ [Å^2][b]	R [Å][c]	ΔE_0 [eV][d]	DFT distance R = H [Å]	DFT distance R = Si(OH)$_3$ [Å]
Initially prepared sample[e]	O	4.0	7.1	2.07	−1.6	2.11	2.15
	C	4.3	7.4	2.21	5.1	2.20	2.21
	C$_l$[f]	1.9	3.9	3.03	−1.2	3.00	3.02
	Al	1.1	5.4	3.08	1.6	3.00	3.03
$^{13}C_6H_6$-treated sample[g]	O	3.3	6.5	2.08	−7.5		2.15,[h] 2.13[i] 2.15,[j] 2.16[k]
	C	6.8	1.3	2.24	−1.4		2.18,[h] 2.19[i] 2.18,[j] 2.18[k]
	Al	1.1	5.2	3.14	−5.1		3.01,[h] 3.02[i] 2.95,[j] 2.98[k]

[a] Coordination number. [b] Sigma-squared value (Debye–Waller factor). [c] Inter-atomic distance. [d] Inner potential correction. [e] Data reported previously.[3c] [f] l = long. [g] Fit in R range $3.54 < k < 11.70$ Å; $0.8 < R < 3.0$ Å. Estimated errors: N ±20%; R ±0.02 Å; $\Delta\sigma^2$ ±20%; ΔE_0 ±10%. Note that the coordination number and distance of the Ru–Al contribution were not determined with as much confidence as other parameters. [h] Figure 5a. [i] Figure 5b. [j] Figure 5c. [k] Figure 5d.

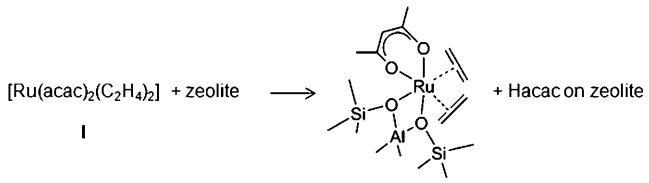

Scheme 1. Reaction of **I** with the zeolite to form a supported ruthenium complex and neutral protonated acac (Hacac) on the zeolite.

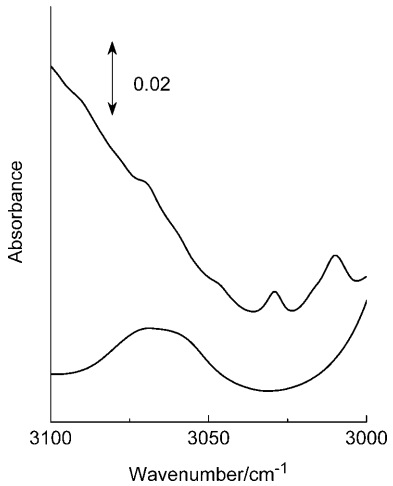

Figure 2. IR spectra in the ν_{CH} region of the initially prepared sample (top) and the $^{13}C_6H_6$-treated sample (bottom). The spectrum of the initially prepared sample has been reported before[3d] and is included here for comparison.

1575 cm^{-1}).[3d,4,7a–c] The $\tilde{\nu}$ = 1521 cm^{-1} band characteristic of the supported sample is blueshifted relative to the $\tilde{\nu}$ = 1515 cm^{-1} band characteristic of **I**.[4] Similar shifts are observed when [Ru(acac)$_3$] is supported on the same zeolite[3d] and when [Au(acac)(CH$_3$)$_2$] is supported on silica.[8] The scaled calculated values for the bands in the range of $\tilde{\nu}$ = 1500 to 1600 cm^{-1} are in satisfactory agreement with the experimental values (within about 10 cm^{-1}). The calculated values for the lower-energy band do not exhibit a shift difference between the characteristic values for **I** and the complex in the zeolite. It has been suggested[7a–c] that the frequencies of characteristic IR bands of acac ligands of supported metal complexes can be influenced by noncovalent interactions between the acac ligands and the support surface, and we infer that our model representing the zeolite may not be large enough to account for such interactions. However, we stress that the shift of 6 cm^{-1} is very small and that previous authors have noted that it is difficult to assign all of the bands in the IR spectra of metal–acac complexes on silica.[7a–c]

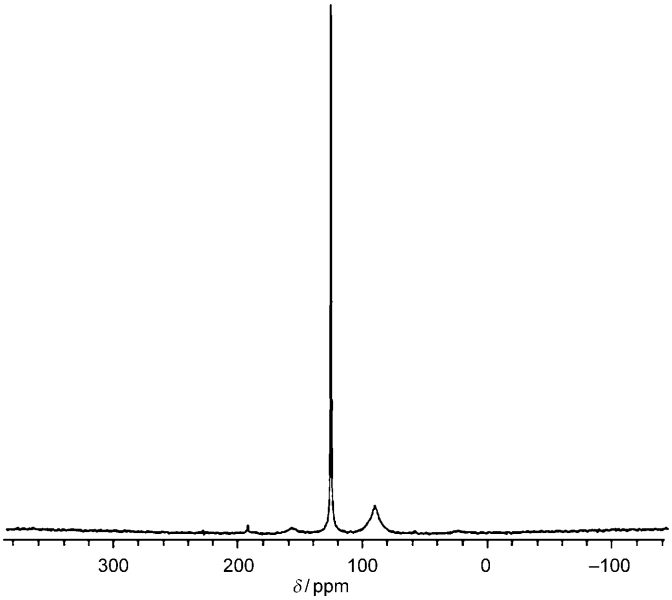

Figure 3. ^{13}C CP/MAS NMR spectrum of the supported ruthenium complex with a benzene ligand.

The spectra also show that the intensities of the bands characteristic of acac ligands bonded at Al sites of the zeolite, presumably as Hacac (at $\tilde{\nu}$ = 1537 and 1590 cm^{-1}),[9] were greater than the intensities of those in the spectrum of the sample prior to treatment with $^{13}C_6H_6$ (Figure 4). The area of the $\tilde{\nu}$ = 1537 cm^{-1} band characteristic of the $^{13}C_6H_6$-treated sample was approximately twice that of the sample before treatment with $^{13}C_6H_6$ (Figure 4).

These results indicate that treatment of the sample with $^{13}C_6H_6$ led to the removal of the ethene and acac ligands from the ruthenium, presumably because they were replaced

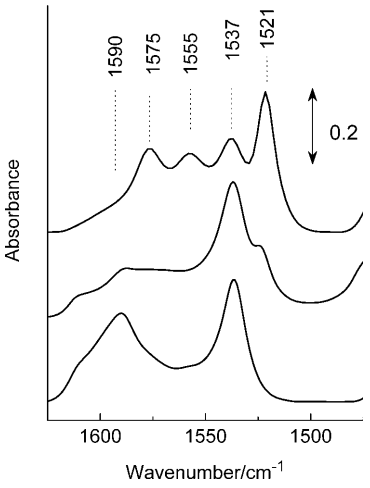

Figure 4. IR spectra of zeolite-supported samples. Top: Initially prepared sample of zeolite-supported ruthenium complex; middle: $^{13}C_6H_6$-treated sample; bottom: acetylacetone adsorbed on the zeolite. The IR spectra were normalized with respect to the IR band characteristic of the zeolite centered at $\tilde{\nu}=1870\ cm^{-1}$.

by $^{13}C_6H_6$ and a negatively charged part of the zeolite that was needed to maintain charge balance.

IR spectra characterizing the treated sample in the ν_{OH} region (Figure S1 in the Supporting Information) also include a broad band at approximately $\tilde{\nu}=3500\ cm^{-1}$, which indicates hydrogen bonding of species formed during the treatment. Because there is no evidence in the IR spectrum of a bending mode of H_2O adsorbed on the zeolite, which would be expected at approximately $\tilde{\nu}=1628\ cm^{-1}$ (Figure S1 in the Supporting Information), we suggest that the broad band is indicative not of water but instead of physisorbed $^{13}C_6H_6$ or protonated acac (Hacac).[10] The structure calculated for Hacac interacting with $Si(OH)_4$ is shown in Figure 1d. The scaled[3e] SiO–H stretching frequency is shifted from approximately $\tilde{\nu}=3765\ cm^{-1}$ to approximately $\tilde{\nu}=3460\ cm^{-1}$, consistent with the observed spectra. The carbonyl group of the Hacac serves as the proton acceptor with an Si–OH being the proton donor, consistent with a previous analysis.[7] The short SiOH···O=C length is 1.78 Å with a binding energy of about 6.0 kcal mol^{-1}.

Ru K edge EXAFS characterization of the treated sample: Further information about the supported ruthenium complexes incorporating benzene ligands is provided by the EXAFS data (Table 2). Fourier transforms of the EXAFS data and best fits of the data with various k weightings are shown in the Supporting Information, Figures S2 and S3. The EXAFS data characterizing the supported ruthenium ethene complex formed by the reaction of the zeolite with **I**, reported earlier,[3d] are included for comparison in Table 2.

The EXAFS data for the complex after treatment with $^{13}C_6H_6$ give no evidence of a Ru–Ru contribution within the expected error (Table 2 and Table S1 in the Supporting Information), which indicates that essentially all ruthenium remained as mononuclear complexes in the zeolite after the $^{13}C_6H_6$ treatment. The EXAFS data do not give evidence of a long Ru–C contribution near 3.0 Å characteristic of acac ligands bonded to the ruthenium, whereas the data characterizing the sample before treatment with $^{13}C_6H_6$ do indicate this contribution (Table 2).[3d]

Thus, the EXAFS data, consistent with the IR data, show that most of the acac and ethene ligands were removed from the ruthenium on treatment with $^{13}C_6H_6$. On the basis of a deconvolution of the IR bands,[3d] we estimate that approximately 85% of the acac ligands were removed.

The EXAFS data characterizing the supported ruthenium–benzene complex also indicate a Ru–O contribution, with a coordination number of approximately three and a bond length in the range expected for Group 8 metal complexes bonded to metal oxides and zeolites (2.08 Å, Table 2).[11] Because the IR and EXAFS data show the removal of acac ligands from ruthenium after the treatment with $^{13}C_6H_6$ (Figure 2, Table 2), the treated ruthenium complexes, on average, need to be bonded to the zeolite through three Ru–O bonds instead of the two present in the initially prepared sample. This result is required to provide a neutral species because of the +2 charge on the Ru. The acidic site of the zeolite and the acac in the original complex provide two negative charges to balance the +2 charge. Loss of the acac ligand means that an additional anionic O in the zeolite must bind to the Ru^{II} ion to balance the charge. This anionic oxygen atom is expected to arise from the site that provides the H^+ to neutralize the acac, as discussed above.

The EXAFS data characterizing the $^{13}C_6H_6$-treated sample also include a Ru–C contribution, with a coordination number of approximately six at a bonding length of 2.24 Å (Table 2). Within the error of the EXAFS analysis, this length is consistent with those characteristic of ruthenium–η^6-benzene complexes that incorporate polyoxometalate ligands (2.106–2.233 Å), which we infer are good models of our zeolite-supported metal complex.[2e–g] The coordination number of approximately six indicates the presence of one η^6-$^{13}C_6H_6$ ligand per Ru atom. The smaller $\Delta\sigma^2$ value for the Ru–C contribution of the sample treated with $^{13}C_6H_6$ ($\Delta\sigma^2=1.3\times10^{-3}$ Å^2) compared with that for the initially prepared sample ($\Delta\sigma^2=7.4\times10^{-3}$ Å^2; Table 2) indicates that the bonds between the Ru atoms and the carbon atoms of the $^{13}C_6H_6$ ligands are more nearly uniform than the bonds between the Ru atoms and the ethene ligands in the initially prepared sample.

The reaction leading to the bonding of $^{13}C_6H_6$ with the Ru centers led to almost no change in the Ru–Al coordination number (with the value being approximately 1), a result that shows that the ruthenium complexes remained bonded to oxygen atoms near the Al sites (these are the charged sites where cationic species are expected to bond). We caution, however, that the Ru–Al coordination number and length are not determined with as much confidence as the other EXAFS parameters. The Ru–Al length of 3.14 Å is only slightly longer than that of the supported ruthenium acac complex from which the supported benzene complex was formed.

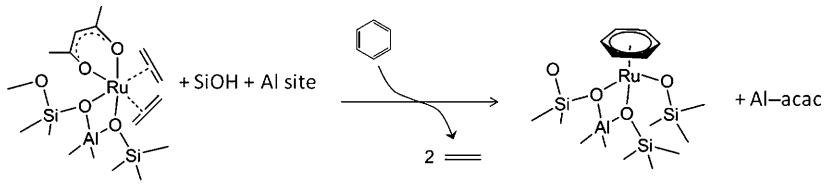

Scheme 2. Treatment of the supported ruthenium complex with benzene to form a supported ruthenium complex with a benzene ligand and protonated acac (Hacac) on zeolite.

In summary, the EXAFS data for the treated sample are consistent with the IR and NMR data and demonstrate replacement of two ethene ligands and one acac ligand with one $^{13}C_6H_6$ ligand per Ru atom, to form a zeolite-supported mononuclear ruthenium complex with an η^6-benzene ligand and with an additional oxygen from the support to balance the charge, as shown in Scheme 2.

Density functional theoretical modeling of supported ruthenium–benzene complex: On the basis of the experimental results and charge conservation models, we developed a number of possible structures for binding an $[Ru^{II}(C_6H_6)]$ complex to the zeolite (Figure 5). The $[Ru(C_6H_6)]$ was anchored to the acidic site of the zeolite $Al(OR)_4$ plus an additional acidic site from a deprotonated silanol group for charge balance, with various connectivities to the acidic site. For the case of $R=Si(OH)_3$, an isolated $OSi(OH)_3$ was attached to Ru^{II} for the charge balance (Figure 5a). The complex represented in Figure 5b is the original $Ru–Al(OH)_4$ model, plus a silanol group connected by three SiO fragments bridging the Ru atom and one of the AlO(H) binding sites to make the SiO^- site. The structure shown in Figure 5c is essentially the same as that shown in Figure 5b, but with the hydrogen atom of the Al-O-H acidic binding site of the latter replaced by $Si(OH)_3$. The structure shown in Figure 5d has the charge-balancing $(O)_2(OH)SiO^-$ site from Figure 5a connected to the $Si(OH)_3$ groups on the $Al(OSiH_3)_4$ by removal of an OH. One of these two oxygen atoms bonded to the Al atom is bonded to the Ru and one is not. We also performed simulations of a $[Ru(acac)(C_6H_6)]$ complex bonded to the acidic $Al(OR)_4^-$ site of the zeolite.

The calculated Ru–O bond lengths (Table 2) are 0.05 to 0.11 Å too long as compared with the experimental (EXAFS) values, with the larger complexes showing a larger discrepancy. The Ru–O bond lengths are not all equal, with the Ru–O(Si–O$^-$) length being 2.03 to 2.06 Å and the Ru–O(acidic site) length being longer at 2.17 to 2.20 Å. This difference is appropriate because a single negative charge is localized on oxygen in the Si–O$^-$ site, and the negative charge on the acidic site is shared by two oxygen atoms. The calculated Ru–C(C_6H_6) bond lengths are too short by 0.06 to 0.09 Å. This result is consistent with the Ru–O bond length being too long because the longer Ru–O bond length means that the Ru atom can better interact with the benzene. The Ru–Al length is calculated to be up to 0.19 Å too short relative to the experimental value. This last length is effectively a measure of the O-Al-O bond angle or the O-Ru-O bond angle, or both of the angles, which are opened up in the model structures. This comparison is not strongly quantitative because the Ru–Al length determined by EXAFS spectroscopy is relatively uncertain, as

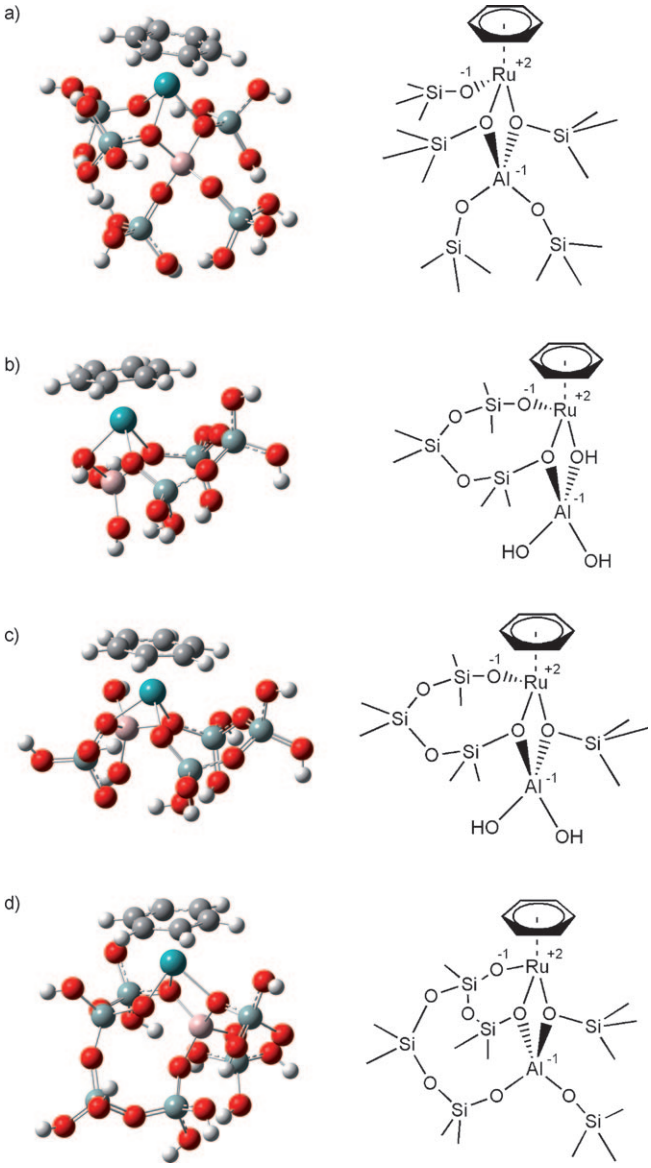

Figure 5. DFT-optimized molecular geometries of $[Ru(C_6H_6)]$ anchored to the acidic $Al(OR)_4$ site of the zeolite plus an additional acidic site from a deprotonated silanol group for charge balance, with various connectivities to the acidic site. a) $R=Si(OH)_3$ plus an isolated $OSi(OH)_3$ for charge balance. b) $Ru–Al(OH)_4$ model plus a silanol group connected by three SiO fragments bridging the Ru atom and one of the AlO(H) binding sites to generate the SiO^- site. c) The structure from Figure 5b with Al-O-$Si(OH)_3$ instead of Al-O-H. d) Charge-balancing $(O)_2(OH)SiO^-$ site from Figure 5a generated by connecting to the $Si(OH)_3$ groups on the $Al(OSiH_3)_4$ by removal of an OH group (structure **III**).

mentioned above. The hapticity of the benzene ring in the complexes in Figure 5 is η^6 because all of the C atoms are approximately equidistant from Ru.

The calculated Mulliken charges on the Ru^{II} are 0.644, 0.587, 0.659, and 0.540 e for Figure 5a–d, respectively. These results suggest that the amount of charge transfer from the additional SiO^- group depends on the structure of the zeolite, with more charge transfer in Figure 5b and d than in 5a and c.

Discussion

Reaction of supported ruthenium complex with $^{13}C_6H_6$

Exchange of ethene and acac ligands with $^{13}C_6H_6$: To better understand the reaction process, we calculated the energetics of the following reaction (Figures 5 and 6):

$$\mathbf{IV}+C_6H_6 \rightarrow \mathbf{III}+2\,C_2H_4+\text{Hacac} \quad (1)$$

The calculated reaction enthalpy is $\Delta H \approx +30$ kcal mol^{-1}, which does not include the interaction of the Hacac with the zeolite. We also calculated the energy of Reaction (2) to be $\Delta H \approx +17$ kcal mol^{-1} (Figures 1 and 6).

$$\mathbf{II}+C_6H_6 \rightarrow \mathbf{V}+2\,C_2H_4 \quad (2)$$

The hapticity of the benzene in **V** is η^2 to η^4, with two short Ru–C bonds averaging 2.20 Å, two averaging 2.38 Å, and two long Ru–C bonds averaging 3.05 Å. The benzene displaces both the acac and the two ethylene molecules because there is not enough space for both an acac and C_6H_6 around Ru as a consequence of the steric constraints present even in our simple model of the active site. We have also calculated the entropy contributions to the reaction energies. For Reaction (2), assuming that the ruthenium complexes are like a solid and have approximately equal entropies, the entropy contributes -12 kcal mol^{-1} to the Gibbs free energy at 298 K, and the entropy contributes -17 kcal mol^{-1} to the Gibbs free energy at 423 K, so that the reaction has an equilibrium constant of $K \approx 1$ at the higher temperature. The entropy change of Reaction (1) would be the same if the Hacac were complexed to the surface. If the Hacac were free, the entropy term at 298 K would contribute -28 kcal mol^{-1} to the free energy of Reaction (1), and so we infer that it is likely that the reaction can occur.

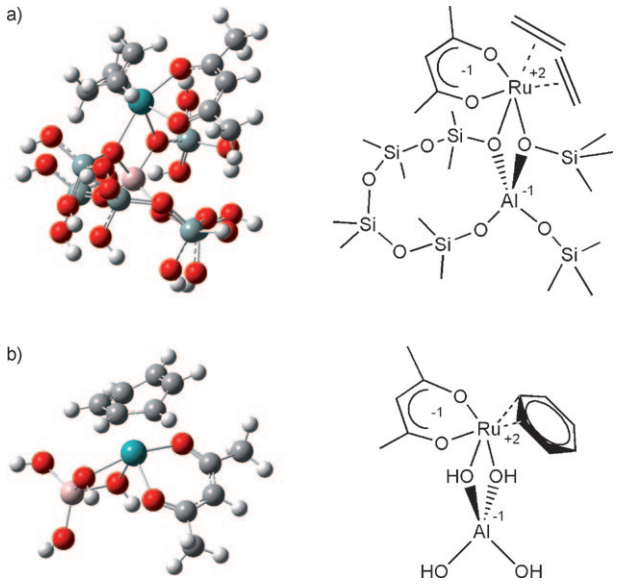

Figure 6. a) Complex **IV** in Reaction (1) and b) complex **V** in Reaction (2).

These energetic results suggest that the interaction of the Hacac with the zeolite is sufficient to provide the additional energy needed for the reaction to proceed. This inference is consistent with the calculated hydrogen-bonding interaction of about 6 kcal mol^{-1} for Hacac with the model compound $Si(OH)_4$. This value could readily be at least 10 kcal mol^{-1}, depending on the exact form of the hydroxyl group. The abstraction by acac of H from an SiOH group on Cab-O-Sil silica with silanol protons has been suggested by White, Mitchell, and co-workers to be an important process for the interaction of metal acac complexes with silica surfaces.[7] These authors reported the likely interaction of the formed Hacac with the silanol groups by hydrogen bonding.[7] Furthermore, these authors suggested that an $Si–O^-$ group could interact with the metal ion in the metal acac complex if the steric interactions were appropriate and if the metal center could adopt a higher valency; for example, square-planar $[Cu(acac)_2]$ forms a surface complex, whereas $[Pd(acac)_2]$ and $[Pt(acac)_2]$ do not.

We also calculated the acidity of Hacac relative to that of $Si(OH)_4$, as shown by Reaction (3).

$$Si(OH)_4+\text{acac} \rightarrow \text{Hacac}+Si(OH)_3O^- \quad (3)$$

The reaction is thermoneutral, showing that acac has about the same acidity as $Si(OH)_4$. The gas-phase acidities of acac and $Si(OH)_4$ are both about 353 kcal mol^{-1}, which makes them moderate acids on the gas-phase acidity scale.[12]

Number of Ru–O bonds anchoring the ruthenium complex to the zeolite after treatment with $^{13}C_6H_6$: The EXAFS data (Table 2) indicate that each ruthenium mono-acac complex in the initially prepared sample was bonded to the zeolite through two Ru–O bonds. After treatment with $^{13}C_6H_6$, the EXAFS data show that each ruthenium complex was bonded to the zeolite through approximately three Ru–O bonds. If we assume that ruthenium remains in a formal oxidation state of +2, the additional oxygen that becomes bonded to Ru during treatment with $^{13}C_6H_6$ needs to be anionic and provide a formal charge of -1 to ruthenium. Because we used a high-silica zeolite, and the EXAFS results indicate that ruthenium complexes remained bonded to Al sites, we infer that the additional oxygen atoms came

from other silanol groups that were not directly bonded to Al sites.

Kenvin et al.[7a] reported that acac ligands of a silica-supported $[Cu(acac)_2]$ complex were dissociated to form Hacac at approximately 423 K and suggested that this reaction occurred by protonation of acac ligands by silanol groups of silica. Van Der Voort et al.[7c] subsequently reported a similar reaction with silica-supported [VO(acac)] complexes. On the basis of these results, we suggest that the acac ligands of our supported ruthenium complexes in the initially prepared sample were removed by reacting with silanol groups that are not associated with Al sites during treatment with $^{13}C_6H_6$ at 413 K, aided by the formation of ruthenium–benzene complexes, as shown in Scheme 2. Most of the Hacac species became bonded to Al sites of the zeolite as shown by the IR data (Figure 4), and we infer that others interacted with each other or with silanol groups of the zeolite through hydrogen bonding, as indicated by the IR spectra shown in Figure S1 in the Supporting Information.

Our EXAFS results indicating that the $[Ru(C_6H_6)]$ species is bonded to three oxygen atoms of the zeolite are supported by crystallographic data characterizing various (presumably analogous) polyoxometalate-supported ruthenium complexes with η^6-C_6H_6 ligands.[2e,f] These literature data show that the $[Ru(C_6H_6)]^{2+}$ moieties in these complexes are bonded to three oxygen atoms each, with bond lengths in the range of approximately 2.003–2.183 Å. For example, the crystal structure of $Rb_2Na_4[\{Ru(C_6H_6)\}_2SiW_9O_{34}]\cdot 21\,H_2O$ reported by Bi et al.[2f] shows $[Ru(C_6H_6)]^{2+}$ moieties bonded to three oxygen atoms of the polyoxometalate, with bond lengths ranging from 2.075 to 2.183 Å and 2.090 to 2.111 Å (there are two $[Ru(C_6H_6)]^{2+}$ moieties per molecule). Our EXAFS data characterizing the zeolite-supported ruthenium complex after treatment with $^{13}C_6H_6$ indicate an average Ru–O bond length of 2.08 Å (Table 1) that is, within the error of EXAFS analysis, in the range of the Ru–O bond lengths characterizing the $[Ru(C_6H_6)]^{2+}$ compounds with polyoxometalate ligands. Our calculated values for the Ru–O bond lengths are also consistent with the crystallographic and EXAFS bond lengths, providing further confirmation of the structure. Moreover, the charge balance is consistent with an additional $Si–O^-$ group bonding to the Ru^{II}–acidic site complex.

Thus, we infer that our supported ruthenium–benzene complex is a close analogue of well-characterized molecular species. This comparison provides a further confirmation that polyoxometalate ligands can serve as good models of a zeolite support, at least in terms of the bonding to the metal.

Conclusion

A well-defined mononuclear ruthenium diethene complex incorporating an acac ligand was anchored to dealuminated zeolite HY by the reaction of **I** with the zeolite. EXAFS and IR spectra show that $[Ru(acac)(C_2H_4)_2]^+$ was bonded at Al sites of the zeolite via two Ru–O bonds. The structural uniformity of the supported sample led to a good agreement between the experimental results and theoretical calculations at the DFT level. When the supported sample was treated with $^{13}C_6H_6$ at 413 K, essentially complete removal of the ethene and acac ligands from the Ru atoms occurred as indicated by the IR spectra. ^{13}C NMR spectra characterizing the treated sample provided further information about $^{13}C_6H_6$, showing that $^{13}C_6H_6$ ligands had become bonded to the Ru atoms. The EXAFS data indicate that the resultant species is a mononuclear ruthenium complex incorporating a single η^6-$^{13}C_6H_6$ ligand, $[Ru(C_6H_6)]^{2+}$, and that this species is bonded at the Al sites of the zeolite through three Ru–O bonds instead of two Ru–O bonds. Theoretical calculations at the DFT level confirmed the structure of the experimentally determined supported ruthenium complex. Furthermore, the DFT calculations indicate that the bonding of Hacac, which dissociates from the supported ruthenium complexes on treatment with $^{13}C_6H_6$ to the zeolite, facilitates the conversion from the supported diethene complex to the supported benzene complex.

Experimental Section

Materials and procedures: Samples were handled with standard air-exclusion techniques, including Schlenk techniques, and stored in a glove box under dry argon; the O_2 and moisture contents in the glove box were less than 0.1 ppm each. Glassware was dried at 373 K overnight prior to use. *n*-Pentane solvent (Fisher Scientific) was purified in chromatographic columns of activated alumina and of Al_2O_3-supported activated copper (MBraun, MB-SPS). $[Ru(acac)_3]$ (ruthenium(III) acetylacetonate; Strem, 99%) was used to synthesize **I** by a reported method.[4] The yield was 43%. The resultant surface species was characterized by a variety of methods described in the sections below. $^{13}C_6H_6$ (Cambridge Isotopes, 99%) was used in some of the syntheses.

Synthesis of zeolite-supported diethene–ruthenium complexes: The supported samples were made by reacting **I** with the zeolite, as follows: The zeolite powder (Zeolyst, CBV760, Si/Al ratio = 30 (atomic)) was calcined by heating in flowing dry O_2 from RT → 773 K over a period of 3 h, held at 773 K under flowing O_2 for 4 h, and subsequently held under vacuum at 773 K for an additional 16 h. The zeolite was then cooled to RT under vacuum and used immediately for preparation of the supported sample. Complex **I** (0.072 g) was added to the calcined zeolite (2.0 g) in a 100 mL Schlenk flask with a stir bar, ultimately giving a solid that contained 1.0 wt% Ru on the zeolite (Ru/Al ≈ 1:6 (atomic)). Freshly distilled *n*-pentane (≈30 mL) was added to this mixture. The mixture was stirred at RT, and **I** was gradually dissolved in the *n*-pentane and transferred to the zeolite, with which it reacted. After 18 h, the *n*-pentane was removed by evacuation, giving a light pink powder that incorporated all the added ruthenium.

The supported ruthenium complex was synthesized as described above (University of California), then a sample was treated with $^{13}C_6H_6$, and ^{13}C NMR experiments were performed on the resulting new material (University of Southern California). Part of this new sample was characterized by IR spectroscopy (University of California), and part was characterized by EXAFS spectroscopy (Stanford Synchrotron Radiation Laboratory (SSRL)).

Spectroscopic characterization of supported ruthenium complexes

IR spectroscopy of supported ruthenium complexes: Approximately 30 mg of the supported sample formed by the reaction of **I** with the zeolite was pressed into a wafer and then loaded into the IR cell (In-Situ Research Institute, South Bend, IN) in the argon-filled glove box. The cell was

sealed and transferred to an IR spectrometer (Bruker IFS 66v) without exposing the sample to air. After the cell had been loaded into the sample chamber of the spectrometer, the chamber was evacuated. With the sample held at RT under dynamic vacuum ($<10^{-4}$ kPa), spectra were collected in transmission mode with a resolution of 2 cm^{-1}. Each spectrum is the average of 64 scans. The spectra were baseline corrected with the OPUS software (Bruker). The $^{13}C_6H_6$-treated sample was characterized by IR spectroscopy in the same way.

X-ray absorption spectroscopy of supported ruthenium complexes: Each of the supported samples mentioned in the preceding section was characterized by X-ray absorption spectroscopy (XAS) at the Ru K edge. The supported sample prior to treatment with $^{13}C_6H_6$ was characterized at beam line 10-2 at the SSRL; the $^{13}C_6H_6$-treated sample was characterized at beam line 2-3 at the SSRL. The storage ring electron energy was 3 GeV. The ring currents were in the range of 50–100 mA.

Si(220) double-crystal monochromators that were detuned by 20–25 % to minimize the effects of higher harmonics in the X-ray beam were used. The mass of each sample was chosen to give an absorbance of between 1.5 and 3.0 calculated at 50 eV above the Ru K absorption edge. Each supported sample was placed in a cell[13] and maintained under vacuum ($<10^{-7}$ kPa) at liquid-nitrogen temperature (77 K) during the data collection.

X-ray intensity data were collected in transmission mode by use of ion chambers mounted on each end of the sample cell. The beam exiting the synchrotron ring passed first through an ion chamber containing N_2, then through the sample cell, an ion chamber containing argon, a cell containing ruthenium foil, and finally an ion chamber containing argon. The purpose of including the ruthenium foil was to allow energy calibration by simultaneous measurement of the absorption of each sample and that of this foil as a standard. Data were measured at values of the wave vector k of up to 13.0 $Å^{-1}$. The first inflection point of the spectrum of the foil was assigned to be 22 117 eV.

^{13}C NMR spectroscopy of the supported ruthenium complex after treatment with $^{13}C_6H_6$: The sample incorporating the supported ruthenium complex after exposure to $^{13}C_6H_6$ was characterized by NMR spectroscopy, as follows: CP/MAS NMR spectra of the samples were acquired at 75 MHz by using a Varian Infinity Plus spectrometer with an MAS spinning rate of 5.0 kHz. The supported sample (300 mg) was loaded into a CAVERN apparatus that contained an MAS NMR rotor in a glove box. Upon sealing of the CAVERN, it was moved to a vacuum line and evacuated, then $^{13}C_6H_6$ was introduced as a vapor at a final pressure of 0.8 kPa, with the pressure being measured by using an MKS barotron gauge. The sample exposed to the labeled benzene was then dropped into the NMR rotor and sealed with a Kel-F end cap before the CAVERN was opened to the atmosphere. The rotor was loaded into a variable-temperature probe and loaded into the NMR instrument, and a spectrum was acquired as the sample was spun at 5 kHz by the use of N_2. The sample was heated to 413 K and held for 10 min, followed by cooling to RT, after which a second spectrum was acquired at RT to ascertain the influence of heating on the supported ruthenium complex.

All carbon spectra were referenced to hexamethylbenzene as an external standard ($\delta = 17.35$ ppm). For the CP acquisition of NMR spectra, a pulse delay of 0.5 s was used along with a spectral width of 50 kHz and a contact time of 2 ms. Each spectrum is the signal-averaged result of 1000 scans, which were processed with 75 Hz of exponential line broadening.

Electronic structure calculations: The electronic structure calculations of models were performed at the density functional theory level. The optimized geometries and frequencies were obtained with the B3LYP exchange-correlation functional[14] and the DZVP2 basis set[15] on all atoms but Ru. For Ru, the aug-cc-pVDZ-PP basis set and corresponding effective core potential were used.[16] These calculations were done with the Gaussian 03 computer program.[17] The NMR chemical shifts were calculated for the various structures with the pure DFT gradient-corrected BLYP exchange-correlation functional[18] and the TZP basis set by using the ADF code.[19] The NMR calculations were performed with the gauge-invariant atomic orbital (GIAO) approach at the DFT level on the basis of developments in the Ziegler group.[20] Scalar relativistic effects were included at the two-component zero-order regular approximation (ZORA) level for these NMR calculations (with inclusion of the mass-velocity and Darwin terms).[21] The standard for the calculations is TMS for both ^{13}C and ^{1}H.

EXAFS data analysis: Analysis of the EXAFS data was carried out with a difference file technique by using the XDAP software.[22] For each spectrum, the average of four scans was processed by fitting a second-order polynomial to the pre-edge region and subtracting this from the entire spectrum; then the background was subtracted from the resultant spectrum by using cubic spline routines. The functional that was minimized and the function used to model the data are reported elsewhere.[22b] Reference backscattering amplitudes and phase shifts were calculated from the crystallographic data for Ru−O and Ru−C contributions of **I** by using the FEFF7 software;[23] a RuAl alloy was used for the Ru−Al contribution. The number of statistically independent data points was obtained by using the Nyquist theorem.[24,22b] The number of optimized parameters was less than the number of statistically independent data points. In the fitting, the coordination number N (representing each contribution), the sigma-squared value (Debye–Waller factor) $\Delta\sigma^2$, the interatomic distance R, and the inner potential correction ΔE_0 were varied until an optimized fit was obtained at each of four k weightings (k^0, k^1, k^2, and k^3). Errors were estimated on the basis of the standard equations.[26]

We used the following procedure to discriminate between candidate models to represent the data. We checked whether the best-fit EXAFS parameters with each model made good physical sense and discarded models with unrealistic EXAFS parameters. We examined fit quality: not just overall goodness of fit but also fits of individual contributions determined by using a difference file technique.[22b] Details such as comparisons of various candidate models and fits of individual shells for the best-fit model are summarized in the Supporting Information. We report only the best-fit model here.

Estimation of the fraction of acac ligands removed from ruthenium as determined from the IR data: The approximate fraction of the acac ligands removed from the supported ruthenium complexes after treatment of the supported sample with $^{13}C_6H_6$ was estimated by analysis of the IR spectra. Each spectrum was normalized with respect to the IR band at $\tilde{\nu} = 1870$ cm^{-1} characteristic of combination and overtone bands of the zeolite framework. Spectra of the supported samples included bands characteristic of acac ligands remaining bonded to ruthenium ($\tilde{\nu} = 1521$, 1555, and 1575 cm^{-1}) and acac ligands removed from ruthenium and thereafter bonded at Al sites of the zeolite ($\tilde{\nu} = 1537$ and 1590 cm^{-1}), as shown previously.[3d] The approximate fraction of acac ligands removed from the ruthenium was estimated by comparing the band-area ratio of (area of $\tilde{\nu} = 1521$ cm^{-1} band)/(area of $\tilde{\nu} = 1521$ cm^{-1} band + area of $\tilde{\nu} = 1537$ cm^{-1} band) before and after treatment with $^{13}C_6H_6$. Deconvolution was carried out by using the Pearson VII model.[26] The fit parameters were optimized by Levenberg–Marquardt iterations.

Acknowledgements

The research was supported by the Department of Energy (DOE), Office of Science, Basic Energy Sciences (grant numbers DE-FG02-04ER15513 at the University of California, DE-FG02-03ER15481 at the University of Alabama, and DE-FG02-04ER15598 at the University of Southern California). We acknowledge beam time and the support of the DOE Division of Materials Sciences for its role in the operation and development of beam lines 10-2 and 2-3 at the Stanford Synchrotron Radiation Laboratory.

[1] G. W. Parshall, S. D. Ittel in *Homogeneous Catalysis: The Applications and Chemistry of Catalysis by Soluble Transition Metal Complexes*, 2nd ed., Wiley-Interscience, New York, **1992**.

[2] a) M. T. Pope, A. Müller, *Angew. Chem.* **1991**, *103*, 56; *Angew. Chem. Int. Ed. Engl.* **1991**, *30*, 34; b) H. Weiner, J. D. Aiken, R. G. Finke, *Inorg. Chem.* **1996**, *35*, 79053; c) J. D. Aiken, R. G. Finke, *J. Mol. Catal. A* **1999**, *145*, 1; d) S. Ozkär, R. G. Finke, *J. Am. Chem.*

Soc. **2002**, *124*, 5796; e) V. Artero, D. Laurencin, R. Villanneau, R. Thouvenot, P. Herson, P. Gouzerh, A. Proust, *Inorg. Chem.* **2005**, *44*, 2826; f) L. H. Bi, U. Kortz, M. H. Dickman, B. Keita, L. Nadjo, *Inorg. Chem.* **2005**, *44*, 7485; g) L. H. Bi, E. V. Chubarova, N. H. Nsouli, M. H. Dickman, U. Kortz, B. Keita, L. Nadjo, *Inorg. Chem.* **2006**, *45*, 8575; h) K. Nomiya, Y. Kasahara, Y. Sado, A. Shinohara, *Inorg. Chim. Acta* **2007**, *360*, 2313; i) K. Kamata, S. Yamaguchi, M. Kotani, K. Yamaguchi, N. Mizuno, *Angew. Chem.* **2008**, *120*, 2441; *Angew. Chem. Int. Ed.* **2008**, *47*, 2407; j) Y. Kikukawa, S. Yamaguchi, K. Tsuchida, Y. Nakagawa, K. Uehara, K. Yamaguchi, N. Mizuno, *J. Am. Chem. Soc.* **2008**, *130*, 5472; k) A. Proust, R. Thouvenot, P. Gouzerh, *Chem. Commun.* **2008**, 1837.

[3] a) J. O. Ehresmann, P. W. Kletnieks, A. Liang, V. A. Bhirud, O. P. Bagatchenko, E. J. Lee, M. Klaric, B. C. Gates, J. F. Haw, *Angew. Chem.* **2006**, *118*, 588; *Angew. Chem. Int. Ed.* **2006**, *45*, 574; b) A. Uzun, V. A. Bhirud, P. W. Kletnieks, J. F. Haw, B. C. Gates, *J. Phys. Chem. C* **2007**, *111*, 15064; c) P. W. Kletnieks, A. J. Liang, R. Craciun, J. O. Ehresmann, D. M. Marcus, V. A. Bhirud, M. M. Klaric, M. J. Haymann, D. R. Guenther, O. P. Bagatchenko, D. A. Dixon, B. C. Gates, J. F. Haw, *Chem. Eur. J.* **2007**, *13*, 7294; d) I. Ogino, B. C. Gates, *J. Am. Chem. Soc.* **2008**, *130*, 13338; e) I. Ogino, B. C. Gates, *Chem. Eur. J.* **2009**, *15*, 6827; f) A. J. Liang, R. Craciun, M. Chen, T. G. Kelly, P. W. Kletnieks, J. F. Haw, D. A. Dixon, B. C. Gates, *J. Am. Chem. Soc.* **2009**, *131*, 8460; g) I. Ogino, B. C. Gates, *J. Phys. Chem. C* **2009**, *113*, 20036.

[4] M. A. Bennett, M. J. Byrnes, A. C. Willis, *Organometallics* **2003**, *22*, 1018.

[5] T. Shimanouchi, *Tables of Molecular Vibrational Frequencies Consolidated Volume I*, NSRDS-NBS 39, National Bureau of Standards, Washington, **1972**.

[6] G. C. Levy, G. L. Nelson, *Carbon-13 Nuclear Magnetic Resonance for Organic Chemists*, Wiley-Interscience, New York, **1972**.

[7] a) J. C. Kenvin, M. G. White, M. B. Mitchell, *Langmuir* **1991**, *7*, 1198; b) M. B. Mitchell, V. R. Chakravarthy, M. G. White, *Langmuir* **1994**, *10*, 4523; c) P. Van Der Voort, M. B. Mitchell, E. F. Vansant, M. G. White, *Interface Sci.* **1997**, *5*, 169.

[8] M. Hisamoto, R. C. Nelson, M. Y. Lee, J. Eckert, S. L. Scott, *J. Phys. Chem. A* **2009**, *113*, 8794.

[9] a) P. Van Der Voort, I. V. Babitch, P. J. Grobet, A. A. Verberckmoes, E. F. Vansant, *J. Chem. Soc. Faraday Trans.* **1996**, *92*, 3635; b) J. Guzman, B. C. Gates, *Langmuir* **2003**, *19*, 3897.

[10] A. Zecchina, F. Geobaldo, G. Spoto, S. Bordiga, G. Ricchiardi, R. Buzzoni, G. Petrini, *J. Phys. Chem.* **1996**, *100*, 16584.

[11] O. Alexeev, B. C. Gates, *Top. Catal.* **2000**, *10*, 273.

[12] a) I. A. Koppel, R. W. Taft, F. Anvia, S.-Z. Zhu, L.-Q. Hu, K.-S. Sung, D. D. DesMarteau, L. M. Yagupolskii, Y. L. Yagupolskii, N. V. Ignat′ev, N. V. Kondratenko, A. Y. Volkonskii, V. M. Vlasov, R. Notario, R. P.-C. Maria, *J. Am. Chem. Soc.* **1994**, *116*, 3047; b) S. G. Lias, J. E. Bartmess, J. F. Liebman, J. L. Holmes, R. D. Levin, G. W. Mallard, *J. Phys. Chem. Ref. Data* **1988**, *17*(Suppl. 1), 1; c) K. E. Gutowski, D. A. Dixon, *J. Phys. Chem. A* **2006**, *110*, 12044.

[13] R. E. Jentoft, S. E. Deutsch, B. C. Gates, *Rev. Sci. Instrum.* **1996**, *67*, 2111.

[14] a) A. D. Becke, *J. Chem. Phys.* **1993**, *98*, 5648; b) C. Lee, W. Yang, R. G. Parr, *Phys. Rev. B* **1988**, *37*, 785.

[15] N. Godbout, D. R. Salahub, J. Andzelm, E. Wimmer, *Can. J. Chem.* **1992**, *70*, 560.

[16] a) K. A. Peterson, D. Figgen, M. Dolg, H. Stoll, *J. Chem. Phys.* **2007**, *126*, 124101; b) K. A. Peterson in *Annual Reports in Computational Chemistry, Vol. 3* (Ed.: D. C. Spellmeyer, R. A. Wheeler), Elsevier, Amsterdam, **2007**.

[17] Gaussian 03, Revision C.02, M. J. Frisch, G. W. Trucks, H. B. Schlegel, G. E. Scuseria, M. A. Robb, J. R. Cheeseman, J. A. Montgomery, Jr., T. Vreven, K. N. Kudin, J. C. Burant, J. M. Millam, S. S. Iyengar, J. Tomasi, V. Barone, B. Mennucci, M. Cossi, G. Scalmani, N. Rega, G. A. Petersson, H. Nakatsuji, M. Hada, M. Ehara, K. Toyota, R. Fukuda, J. Hasegawa, M. Ishida, T. Nakajima, Y. Honda, O. Kitao, H. Nakai, M. Klene, X. Li, J. E. Knox, H. P. Hratchian, J. B. Cross, V. Bakken, C. Adamo, J. Jaramillo, R. Gomperts, R. E. Stratmann, O. Yazyev, A. J. Austin, R. Cammi, C. Pomelli, J. W. Ochterski, P. Y. Ayala, K. Morokuma, G. A. Voth, P. Salvador, J. J. Dannenberg, V. G. Zakrzewski, S. Dapprich, A. D. Daniels, M. C. Strain, O. Farkas, D. K. Malick, A. D. Rabuck, K. Raghavachari, J. B. Foresman, J. V. Ortiz, Q. Cui, A. G. Baboul, S. Clifford, J. Cioslowski, B. B. Stefanov, G. Liu, A. Liashenko, P. Piskorz, I. Komaromi, R. L. Martin, D. J. Fox, T. Keith, M. A. Al-Laham, C. Y. Peng, A. Nanayakkara, M. Challacombe, P. M. W. Gill, B. Johnson, W. Chen, M. W. Wong, C. Gonzalez, J. A. Pople, Gaussian, Inc., Wallingford CT, **2004**.

[18] A. D. Becke, *Phys. Rev. A* **1988**, *38*, 3098.

[19] a) G. te Velde, F. M. Bickelhaupt, E. J. Baerends, C. Fonseca Guerra, J. A. van Gisbergen, J. G. Snijders, T. Ziegler, *J. Comput. Chem.* **2001**, *22*, 931; b) see also: ADF 2004.01, ADF Users Guide, http://www.scm.com, SCM, Theoretical Chemistry, Vrije Universiteit, Amsterdam.

[20] a) G. Schreckenbach, T. Ziegler, *J. Phys. Chem.* **1995**, *99*, 606; b) G. Schreckenbach, T. Ziegler, *Int. J. Quantum Chem.* **1997**, *61*, 899; c) S. K. Wolff, T. Ziegler, *J. Chem. Phys.* **1998**, *109*, 895; d) S. K. Wolff, T. Ziegler, E. van Lenthe, E. J. Baerends, *J. Chem. Phys.* **1999**, *110*, 7689.

[21] a) E. van Lenthe, E. J. Baerends, J. G. Snijders, *J. Chem. Phys.* **1993**, *99*, 4597; b) J. Autschbach, T. Ziegler in *Calculation of NMR and EPR Parameters: Theory and Application* (Eds.: M. Kaupp, M. Buhl, V. G. Malkin), Wiley-VCH, Weinheim, **2004**, pp. 249–264.

[22] a) M. Vaarkamp, J. C. Linders, D. C. Koningsberger, *Physica B+C* **1995**, *209*, 159; b) D. C. Koningsberger, B. L. Mojet, G. E. van Dorssen, D. E. Ramaker, *Top. Catal.* **2000**, *10*, 143.

[23] S. I. Zabinsky, *Phys. Rev. B: Condens. Matter Mater. Phys.* **1995**, *52*, 2995.

[24] E. A. Stern, *Phys. Rev. B* **1993**, *48*, 9825.

[25] *Error Reporting Recommendations: A Report of the Standards and Criteria Committee, Adopted by the International XAFS Society*, http://ixs.iit.edu/subcommittee_reports/sc/err-rep.pdf.

[26] L. Chen, M. Garland, *Appl. Spectrosc.* **2003**, *57*, 331.

Received: February 4, 2010
Published online: June 10, 2010

